PHYSICAL REVIEW B **95**, 140101(R) (2017)

# Stable high-pressure phases in the H-S system determined by chemically reacting hydrogen and sulfur

Alexander F. Goncharov,[1,2] Sergey S. Lobanov,[2,3] Vitali B. Prakapenka,[4] and Eran Greenberg[4]

[1]*Key Laboratory of Materials Physics, Institute of Solid State Physics, Chinese Academy of Sciences, Hefei 230031, China*
[2]*Geophysical Laboratory, Carnegie Institution of Washington, Washington, D.C. 20015, USA*
[3]*Sobolev Institute of Geology and Mineralogy, Siberian Branch Russian Academy of Sciences, 3 Prospekt Akademika Koptyga, Novosibirsk 630090, Russia*
[4]*Center for Advanced Radiations Sources, University of Chicago, Chicago, Illinois 60637, USA*

(Received 5 February 2017; revised manuscript received 21 March 2017; published 10 April 2017)

Synchrotron x-ray diffraction and Raman spectroscopy have been used to study the chemical reactions of molecular hydrogen ($H_2$) with sulfur (S) at high pressures. We find theoretically predicted $Cccm$ and $Im\bar{3}m$ $H_3S$ to be the reaction products at 50 and 140 GPa, respectively. $Im\bar{3}m$ $H_3S$ is a stable crystalline phase above 140 GPa and it transforms to $R3m$ $H_3S$ on pressure release below 140 GPa. The latter phase is (meta)stable down to at least 70 GPa where it transforms to $Cccm$ $H_3S$ upon annealing ($T < 1300$ K) to overcome the kinetic hindrance. $Cccm$ $H_3S$ has an extended structure with symmetric hydrogen bonds at 50 GPa, and upon decompression it experiences a transformation to a molecular mixed $H_2S$-$H_2$ structure below 40 GPa without any apparent change in the crystal symmetry.

DOI: 10.1103/PhysRevB.95.140101

Superconductivity at temperatures close to 200 K in the H-S system at high pressures ($P$) has been recently reported [1,2]. This discovery attracted a great deal of excitement and stimulated a number of experimental and theoretical studies. The key question is clearly about the mechanism of superconductivity, where a conventional electron-phonon coupling scenario [2–6] is challenged by more exotic (complex) theories [7–9]. However, experimental reports on the properties relevant to superconductivity remain scarce [1,2,10–12], making it difficult to clarify this discussion.

Notably, the high-pressure chemical structure and the stable composition of materials in the H-S system remain under debate. Indeed, while many theoretical studies consider $Im\bar{3}m$ $H_3S$ as the superconducting phase near 150 GPa, there are other reports that challenge the decomposition scenario of $H_2S$ [13] or suggest a compound with a modified crystal chemistry SH-$H_3S$ [14]. X-ray diffraction (XRD) experiments on a starting material of $H_2S$ to 140 GPa at 295 K reported a mixture of phases, where $R3m$ (a lower $P$ modification of $Im\bar{3}m$) $H_3S$ was a minor phase, but it could not be identified uniquely due the absence of characteristic XRD peaks [15]. Likewise, XRD experiments on $H_2S$ compressed at about 180 K [11,12] confirmed the stability of $Im\bar{3}m$ $H_3S$ but in a phase mixture, where the presence of H-S compounds with other compositions could be substantial, likely affecting the superconducting transition temperature ($T_C$) [16]. Most recently, experiments which employed direct elemental synthesis [17] reported only the $Cccm$ $H_3S$ phase up to 160 GPa, thus challenging the theory-based view of the superconducting phase ($Im\bar{3}m$), and suggested it to be metastable.

Experiments aiming to uncover the properties of the H-S system related to superconductivity have to be performed at high pressures approaching 150 GPa, which is challenging because the sample dimensions are necessarily small ($<50$ $\mu$m linear and $<10$ $\mu$m thick). In addition to this, the sample prepared following the recipes of Ref. [2] are multiphase in nature [11,12], making it difficult to draw definitive conclusions about the structure, vibrational properties, conductivity, optical, and other properties. Here, we present the synthesis of $H_3S$ materials performed out of elemental reagents, sulfur and molecular hydrogen (see also Ref. [17]). We show that first-principles theoretical studies of structure and composition [3,12,15,18–20] correctly predict the $Im\bar{3}m$ ($R3m$) $H_3S$ compound as the most stable at 110–150 GPa (cf. Ref. [17]); thus, our work resolves the controversy about the superconducting phase in the H-S system.

We performed the experiments in laser-heated diamond anvil cells (DACs) with 50–300 $\mu$m central culets. Small pieces of single-crystal S were positioned in a hole in a rhenium gasket and filled with $H_2$ gas at $\sim$150 MPa. Subsequently, loaded DACs were cooled down to approximately 180 K, brought to a desired pressure (approximately 50 and 150 GPa), and laser heated, while the anvils were kept at a low temperature near 180 K [12,21]. This $P$-$T$ path was chosen to avoid diamond failure due to the penetration of hydrogen into the diamond anvils, as is often the case in DAC experiments on hydrogen. Successive laser heating of the synthesized $H_3S$ compounds was also performed at room temperature when needed. Synchrotron XRD measurements at GSECARS, APS, ANL [22] with an x-ray beam spot size as small as $3 \times 4$ $\mu$m were used to probe the physical and chemical states of the sample. The vibrational properties of $H_3S$ and the chemical composition of the samples were probed on decompression offline (at HPSynC and Geophysical Laboratory). Pressure was measured using the Au XRD standard [23] (where available), the Raman shift of the stressed diamond [24], and the frequency of the $H_2$ vibron [25]. Two experiments up to 150 GPa showed identical results: A cubic bcc-like $Im\bar{3}m$ phase was synthesized after laser heating ($<1300$ K) at 190 and 295 K. Small amounts of $R3m$ S were preserved in the cavity. Figure 1(a) presents the XRD results at the sample position where the contributions from sulfur and rhenium hydride (formed at the gasket/sample interface) were minimized. The formation of a bcc S lattice in $H_3S$ is clearly seen with the lattice parameter [$a = 3.100(5)$Å at 140(5) GPa], which is very close to the theoretically calculated value of $a = 3.088$ Å

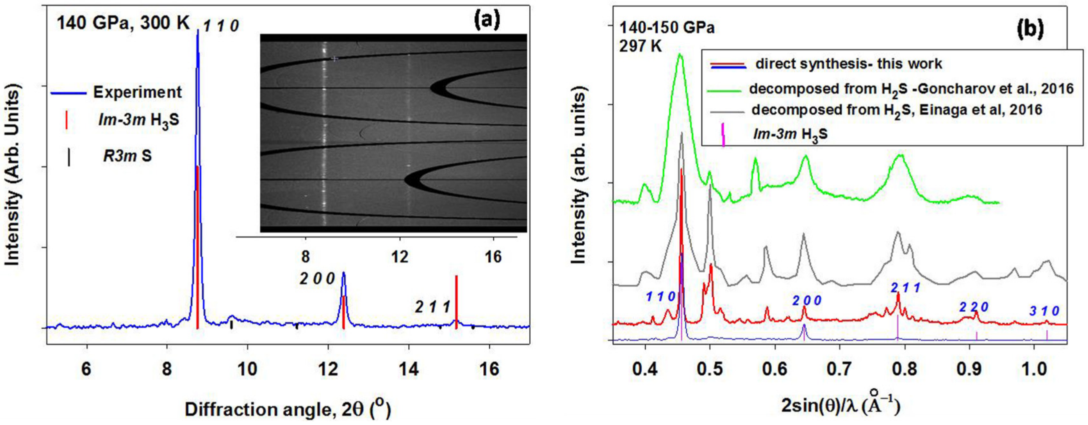

FIG. 1. (a) XRD patterns of $Im\bar{3}m$ $H_3S$ directly synthesized from $H_2$ and S. The x-ray wavelength is 0.3344 Å. The inset is the raw diffraction image in the rectangular coordinates (cake plot). (b) Comparison of the diffraction patterns of $H_3S$-rich materials prepared by different techniques: direct synthesis (two different experiments are shown in red and blue) (this work) and from the $H_2S$ precursor [11,12]. The patterns are plotted as a function of $2\sin\theta/\lambda$, where $\theta$ is the diffraction angle and $\lambda$ is the x-ray wavelength.

for $Im\bar{3}m$ $H_3S$ (e.g., Ref. [3]). The Raman spectra of this phase did not yield any measurable signal, in agreement with the Raman selection rules for $Im\bar{3}m$ $H_3S$ predicting zero Raman-active modes. Please note that the diffraction lines of $Im\bar{3}m$ $H_3S$ synthesized from S and H are very narrow, and much sharper than those observed before in experiments where $H_2S$ was the initial reactant [11,12] [Fig. 1(b)]. Given the perfect agreement between the positions of the observed and predicted Bragg peaks, we conclude that $Im\bar{3}m$ $H_3S$ was synthesized following both reaction pathways, but it is much better crystallized in the case of direct synthesis from the elemental components. We tentatively explain this by a very large diffusivity of hydrogen, which was in excess in this process. In contrast, the synthesis of $H_3S$ out of $H_2S$ occurs at the conditions of hydrogen deficiency, which may suppress the formation of a high-quality sample even with laser annealing. The explanation of this broadening of the diffraction lines has been given in terms of the Magnéli phases—interpenetrating metastable phases of variable composition on a microscopic scale [26]. Unlike previous studies, here we demonstrate the synthesis of a perfectly crystallized $Im\bar{3}m$ $H_3S$.

Unloading of our synthesized $Im\bar{3}m$ $H_3S$ was performed at room temperature, monitoring both XRD and Raman spectra. We find that the Bragg peaks split on unloading down to 120 and 138 GPa in two different experiments. The diffraction peak positions match well $R3m$ $H_3S$ [Fig. 2(a)], however, the distortion of this rhombohedral structure is much larger than that predicted theoretically [3] [Fig. 2(b)]. The splitting of the (110) has been also observed in a previous investigation of $H_3S$ prepared from $H_2S$ [11] (albeit much less clearly), where $Im\bar{3}m$ ($R3m$) $H_3S$ was observed to be metastable down to 92 GPa. The transformation to the $R3m$ structure on unloading was proposed based on the decline of $T_C$, but the authors of Ref. [11] found no evidence of a phase transition in their XRD patterns. Our XRD measurements on directly synthesized $Im\bar{3}m$ $H_3S$ show a rhombohedral

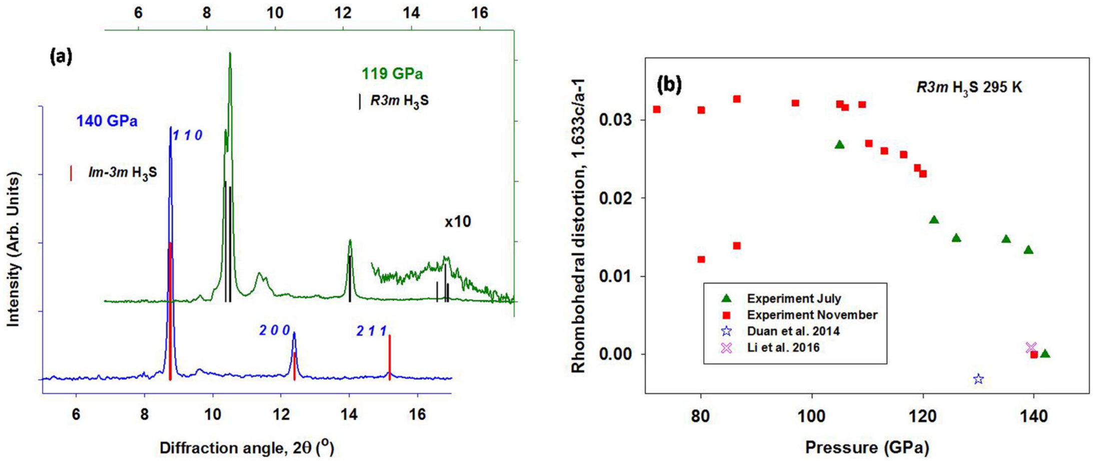

FIG. 2. (a) XRD patterns of $Im\bar{3}m$ $H_3S$ directly synthesized from $H_2$ and S and of $R3m$ $H_3S$ measured on pressure release of the same sample. The x-ray wavelength is 0.3344 Å. Please note the different horizontal axes for the top and the bottom traces. (b) The rhombohedral distortion of $R3m$ $H_3S$ measured in two experiments $r = \sqrt{8/3}c/a - 1$, where $a$ and $c$ are the lattice parameters in the hexagonal setting. A variety of distortions has been observed below 90 GPa depending on the observation points.

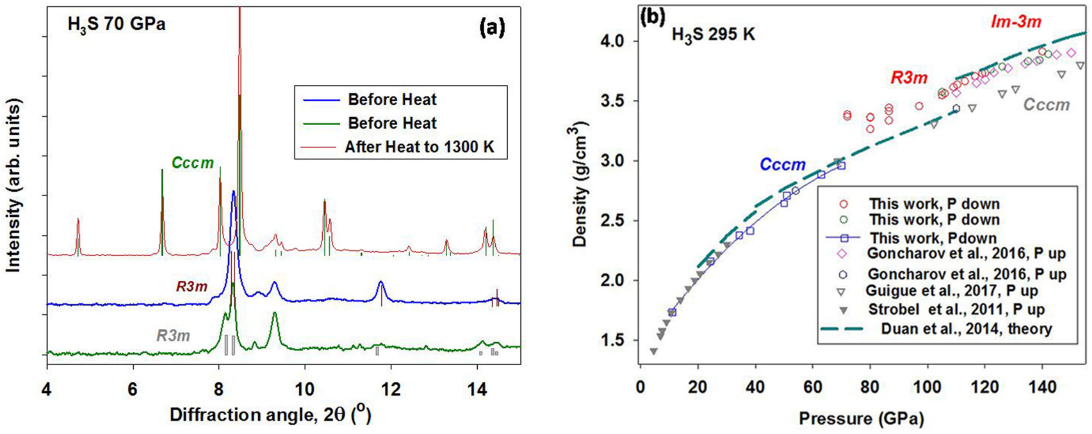

FIG. 3. (a) XRD patterns of *R*3*m* $H_3S$ at 70 GPa before laser heating in two sample positions in comparison to the pattern of *Cccm* $H_3S$ synthesized after heating. The x-ray wavelength is 0.3344 Å. (b) The density of various structural modifications of $H_3S$ as a function of pressure measured in the experiments of this work in comparison to those reported in other experiments [12,17,28] and calculated theoretically [3].

distortion $r = \sqrt{8/3}\,c/a - 1$ increasing first with a pressure decrease and then leveling at a value of 0.03 below 110 GPa [Fig. 2(b)]. Please note that the diffraction peaks measured in this work are much narrower than in a previous study [11], so we believe that our observations of $r$ are not in disagreement. These results challenge the theory predicting a very small rhombohedral distortion. Alternatively, the observed splitting may be due to nonhydrostatic pressure conditions upon pressure release. However, we note that two experiments with a very different hydrogen content in the DAC chamber yielded very similar results, suggesting that these observations are characteristic of *R*3*m* $H_3S$. No Raman activity has been detected in this phase, although one would expect many Raman-active modes due to the asymmetry of the hydrogen bonds in *R*3*m* $H_3S$ [27]. However, *R*3*m* $H_3S$ is predicted to be metallic [3,11] (we also observed the sample to strongly reflect visible light at these conditions, i.e., it appeared to be shiny), which makes these modes weak and thus difficult to detect.

Below 100 GPa or so we find a weakening and broadening of the diffraction peaks assigned to *R*3*m* $H_3S$ and also large variations in the value of the splitting depending on the probed sample area [Figs. 2(b) and 3(a)]. The sample densities [Fig. 3(b)] show a large scattering in values that deviated from the monotonous decompression trend. At approximately 70 GPa we again laser heated the sample below 1300 K and found it to transform instantaneously to another phase, which was clearly identified as *Cccm* $H_3S$, previously predicted theoretically [3] and observed in several different experimental arrangements [12,17,28]. These include its formation at low pressures from the gas phases [28], the chemical reaction of $H_2S$ by laser heating at 55 and 110 GPa [14], and synthesis from S and $H_2$ at 75–100 GPa [17]. Here, we found yet another path–phase transformation of *R*3*m* $H_3S$ on unloading. Previously we had reported on the *Cccm*-to-*R*3*m* transition in $H_3S$ (rather sluggish) [12] on a pressure increase at 295 K that occurred above 110 GPa covering a large phase coexistence range up to 150 GPa.

Three experiments were performed to investigate the pressure-dependent properties of *Cccm* $H_3S$ synthesized directly from $H_2$ and S. In one of these runs, we continued unloading the sample traversing the *R*3*m*-*Cccm* transition as described above following decompression-induced changes in the Raman spectra. In the other two, we documented a direct synthesis of *Cccm* $H_3S$ at approximately 50 and 60 GPa, independently complementing the observations of Ref. [17] at higher pressures [Fig. 3(b)]. In one of these two experiments we managed to concomitantly measure XRD and Raman spectra on unloading. XRD measurements show that the *Cccm* $H_3S$ structure adequately describes the data down to 10 GPa, and we found no irregularities in the equation of state (EOS) [Fig. 3(b)]. However, we found substantial changes in the Raman spectra at 17 and 40 GPa (Fig. 4), at which molecular ordering and/or orientations were modified. At 17 GPa, in parallel to the previous observations of Ref. [28], the S-H and H-H stretching modes split, suggesting orientational ordering of $H_2S$ and $H_2$ molecular units in the structural modification *Cccm*-II. In addition to this, above 40 GPa we found a drastic decrease in intensity and a reduction in the number of observed S-H and H-H stretching modes down to one of each (Fig. 4). Concomitantly, we observed a visual change in the sample appearance: It became shiny in the reflected light. It is interesting that the low-frequency spectra of all three modifications of *Cccm* $H_3S$ are similar, yielding just one weakly pressure-dependent band at approximately 500 $\mathrm{cm}^{-1}$. At above 40 GPa this mode dominates in the Raman spectra, in agreement with our previous report [12], where we synthesized *Cccm* $H_3S$ from $H_2S$.

Our experiments provide strong evidence for the pressure-induced destabilization of $H_2S$ in favor of $H_3S$ as well as the theoretically predicted sequence of the phase transitions *Cccm*-*R*3*m*-$Im\bar{3}m$ $H_3S$ [3], in order of increasing pressure. We found that *Cccm* $H_3S$ is stable in a wide pressure range (see also Ref. [17]), but unlike the observations of Ref. [17], we found that $Im\bar{3}m$ $H_3S$ is stable in the limit of high pressures (140 GPa). This has been demonstrated in two different experimental arrangements: in the direct synthesis presented here of $Im\bar{3}m$ $H_3S$ from $H_2$ and S (two experiments), and also in the *Cccm*-to-$Im\bar{3}m$ transformation observed at 295 K in the experiments where $H_2S$ was a reactant [12].

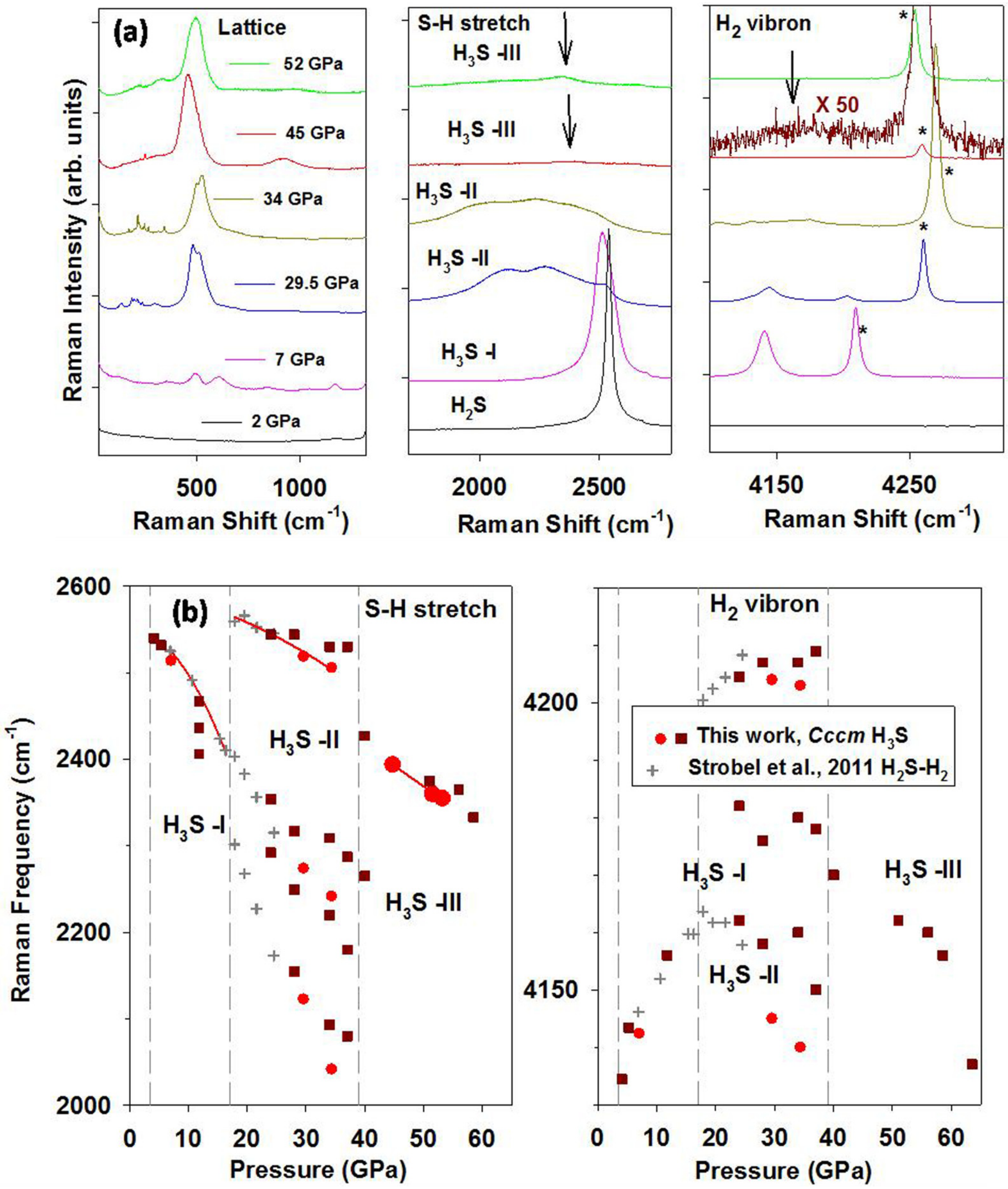

FIG. 4. (a) Raman spectra of *Cccm* $H_3S$ measured on pressure unloading. The excitation wavelength is 532 nm. The asterisks mark the vibron of pure $H_2$; the arrows mark weak peaks. (b) The pressure dependence of the Raman frequencies of *Cccm* $H_3S$ as a function of pressure. The results of this work are compared to those of Ref. [28].

The discrepancy in the phase relation is likely due to a very large stability/metastability range of *Cccm* $H_3S$. Unlike the work reported in Ref. [17], we have synthesized $Im\bar{3}m$ $H_3S$ directly from $H_2$ and S at 140 GPa. In the experiments [11,12], low crystallinity $Im\bar{3}m$ $H_3S$ was synthesized from a heterogeneous disperse phase mixture (which included *Cccm* $H_3S$) for which it was likely easier to overcome the kinetic barrier of transformation.

As predicted theoretically [3,27], superconducting $Im\bar{3}m$ $H_3S$, which has symmetric hydrogen bonds, breaks symmetry at lower pressures, yielding $R3m$ $H_3S$, but the distortion is quite small. On the contrary, our experiments demonstrate quite a large distortion, whose mechanism is unclear. It is likely that this distortion, along with the symmetry breaking, contributes to the decline in superconductivity reported in Ref. [11].

Our observations of an additional modification of *Cccm* $H_3S$ (III) above 40 GPa is likely related to a possible band-gap closure of this material under pressure that was suggested to occur at 110 GPa [3]. Our Raman results (Fig. 4) suggest that this transformation must be also coupled to a subtle structural modification, where two crystallographically different $H_2$ molecules become identical or indistinguishable vibrationally. All three *Cccm* modifications show lower $H_2$ vibron frequencies compared to those of pure molecular $H_2$ [and a very broadened band in *Cccm*-III, Fig. 4(a)], suggesting that an association with the $H_2S$ molecules [28] persists up to high pressures (up to 60 GPa). It is interesting that the high-pressure modification *Cccm*-III $H_3S$ has a single S-H stretching mode. Based on all these observations, we speculate that the formation of *Cccm*-III is associated with a hydrogen bond symmetrization within the $H_2S$ subsystem (e.g., Ref. [29]) transforming the molecular host-guest $H_2S - H_2$ to an extended structure. The low-frequency mode at 500 $cm^{-1}$, which shows a slight redshift in *Cccm*-III, represents the vibrations of tetrahedrally coordinated S.

In conclusion, we have synthesized all three theoretically predicted high-pressure modifications of $H_3S$ at pressures that correlate well with the superconducting properties. Unlike the previously reported synthesis of $H_3S$ by the decomposition of $H_2S$, a direct synthesis from $H_2$ and S results in the formation of pure $H_3S$. We suggest that the superconducting properties of the directly synthesized $H_3S$ should be examined as such a prepared material has a much better crystallinity compared to that obtained by $H_2S$ decomposition.

A.F.G. was partly supported by the Chinese Academy of Sciences visiting professorship for senior international scientists (Grant No. 2011T2J20) and Recruitment Program of Foreign Experts. A.F.G. and V.P. are grateful to the NSF MRI EAR/IF1531583 award. S.L. was partly supported by state assignment project No. 0330-2016-0006. GSECARS is supported by the US NSF (EAR-1128799, DMR-1231586) and DOE Geosciences (DE-FG02-94ER14466). Use of the APS was supported by the DOE-BES under Contract No. DE-AC02-06CH11357. We thank Maddury Somayazulu, Viktor Struzhkin, and Xia-Jia Chen for useful suggestions and Cheng Ji, Dave Mao, and Rich Ferry for enabling the Raman measurements at HPSynC, APS.

---

[1] A. P. Drozdov, M. I. Eremets, and I. A. Troyan, arXiv:1412.0460.

[2] A. P. Drozdov, M. I. Eremets, I. A. Troyan, V. Ksenofontov, and S. I. Shylin, Nature (London) **525**, 73 (2015).

[3] D. Duan, Y. Liu, F. Tian, D. Li, X. Huang, Z. Zhao, H. Yu, B. Liu, W. Tian, and T. Cui, Sci. Rep. **4**, 6968 (2014).

[4] N. Bernstein, C .S. Hellberg, M. D. Johannes, I. I. Mazin, and M. J. Mehl, Phys. Rev. B **91**, 060511 (2015).

[5] D. A. Papaconstantopoulos, B. M. Klein, M. J. Mehl, and W. E. Pickett, Phys. Rev. B **91**, 184511 (2015).

[6] Y. Li, J. Hao, H. Liu, Y. Li, and Y. Ma, J. Chem. Phys. **140**, 174712 (2014).

[7] A. P. Durajski, Sci. Rep. **6**, 38570 (2016).

[8] A. Bianconi and T. Jarlborg, Novel Supercond. Mater. **1**, 37 (2015).

[9] J. E. Hirsch and F. Marsiglio, Physica C **511**, 45 (2015).

[10] I. Troyan, A. Gavriliuk, R. Rüffer, A. Chumakov, A. Mironovich, I. Lyubutin, D. Perekalin, A. P. Drozdov, and M. I. Eremets, Science **351**, 1303 (2016).

[11] M. Einaga, M. Sakata, T. Ishikawa, K. Shimizu, M. I. Eremets, A. P. Drozdov, I. A. Troyan, N. Hirao, and Y. Ohishi, Nat. Phys. **12**, 835 (2016).

[12] A. F. Goncharov, S. S. Lobanov, I. Kruglov, X. -M. Zhao, X.-J. Chen, A. R. Oganov, Z. Konôpková, and V. B. Prakapenka, Phys. Rev. B **93**, 174105 (2016).

[13] S. Duwal and C.-S. Yoo, J. Phys. Chem. C **120**, 21770 (2016).

[14] E. E. Gordon, K. Xu, H. Xiang, A. Bussmann-Holder, R. K. Kremer, A. Simon, J. Köhler, and M.-H. Whangbo, Ang. Chem. **55**, 3682 (2016).

[15] Y. Li, L. Wang, H. Liu, Y. Zhang, J. Hao, C. J. Pickard, J. R. Nelson, R. J. Needs, W. Li, Y. Huang, I. Errea, M. Calandra, F. Mauri, and Y. Ma, Phys. Rev. B **93**, 020103 (2016).

[16] R. Akashi, M. Kawamura, S. Tsuneyuki, Y. Nomura, and R. Arita, Phys. Rev. B **91**, 224513 (2015).

[17] B. Guigue, A. Marizy, and P. Loubeyre, Phys. Rev. B **95**, 020104 (2017).

[18] D. Duan, X. Huang, F. Tian, D. Li, H. Yu, Y. Liu, Y. Ma, B. Liu, and T. Cui, Phys. Rev. B **91**, 180502 (2015).

[19] J. A. Flores-Livas, A. Sanna, and E. K. U. Gross, Eur. Phys. J. B **89**, 63 (2016).

[20] I. Errea, M. Calandra, C. J. Pickard, J. Nelson, R. J. Needs, Y. Li, H. Liu, Y. Zhang, Y. Ma, and F. Mauri, Phys. Rev. Lett. **114**, 157004 (2015).

[21] V. V. Struzhkin, D. Y. Kim, E. Stavrou, T. Muramatsu, H.-K. Mao, C. J. Pickard, R. J. Needs, V. B. Prakapenka, and A. F. Goncharov, Nat. Commun. **7**, 12267 (2016).

[22] V. B. Prakapenka, A. Kubo, A. Kuznetsov, A. Laskin, O. Shkurikhin, P. Dera, M. L. Rivers, and S. R. Sutton, High Press. Res. **28**, 225 (2008).

[23] Y. Fei, A. Ricolleau, M. Frank, K. Mibe, G. Shen, and V. Prakapenka, Proc. Natl. Acad. Sci. USA **104**, 9182 (2007).

[24] Y. Akahama and H. Kawamura, J. Appl. Phys. **100**, 043516 (2006).

[25] H.-K. Mao and R. J. Hemley, Rev. Mod. Phys. **66**, 671 (1994).

[26] R. Akashi, W. Sano, R. Arita, and S. Tsuneyuki, Phys. Rev. Lett. **117**, 075503 (2016).

[27] I. Errea, M. Calandra, C. J. Pickard, J. R. Nelson, R. J. Needs, Y. Li, H. Liu, Y. Zhang, Y. Ma, and F. Mauri, Nature (London) **532**, 81 (2016).

[28] T. A. Strobel, P. Ganesh, M. Somayazulu, P. R. C. Kent, and R. J. Hemley, Phys. Rev. Lett. **107**, 255503 (2011).

[29] A. F. Goncharov, V. V. Struzhkin, H.-K. Mao, and R. J. Hemley, Phys. Rev. Lett. **83**, 1998 (1999).